

Continuum models for surface growth

Martin Rost

Abstract. As an introductory lecture to the workshop an overview is given over continuum models for homoepitaxial surface growth using partial differential equations (PDEs). Their *heuristic derivation* makes use of inherent symmetries in the physical process (mass conservation, crystal symmetry, . . .) which determines their *structure*. Two examples of applications are given, one for large scale properties, one including crystal lattice discreteness. These are: (i) a simplified model for *mound coarsening* and (ii) for the transition from *layer-by-layer* to *rough growth*. Virtues and shortcomings of this approach is discussed in a concluding section.

Mathematics Subject Classification (2000). Primary 99Z99; Secondary 00A00.

Keywords. Class file, journal.

1. Introduction

Crystal growth by Molecular Beam Epitaxy (MBE) involves processes on quite different physical scales, from atomic to micrometer scales. To capture the large scale features it may be appropriate to represent the surface as a continuous height field $h(\mathbf{x}, t)$ above a set of so called base points \mathbf{x} where $h : (\mathbf{x}, t) \in \mathbb{R}^2 \times \mathbb{R} \rightarrow \mathbb{R}$. The surface dynamics is then modelled by a parabolic PDE for $h(\mathbf{x}, t)$, which often is a starting point interesting mathematical problems, and in some cases for rigorous results [8, 9], which were an important part of this workshop.

Their mathematical tractability somehow contrasts with the lack of rigour in their derivations, as we shall see below. It would be nice to “prove” a certain PDE to be the appropriate large scale model for some underlying more elementary model, typically a stochastic model of the solid-on-solid type. This would connect the result for large scales with the microscopic model which is much closer to physical reality.

Nevertheless, often this chain can be closed in a heuristic sense, and this lecture presents some examples. It is organised as follows: First, the heuristic procedure of deriving a continuum model is motivated and its structure is explained.

Then, two examples of applications are presented, covering in some sense extreme cases of applicability of continuum models; (i) coarsening of mound patterns in homoepitaxy and (ii) damping of width oscillations in the transition from layer-by-layer to rough growth. Last, the general applicability of continuum models to MBE growth is discussed, in particular those features of discreteness of the underlying process which can only be covered incompletely by a continuum model. Open questions in the derivation which have not been addressed so far, but appear to be solvable, are mentioned here.

The main purpose of this introductory lecture is to recollect the physical motivation of the class of models which deal with the largest spatial and temporal scales involved in MBE growth, and to give some intuition to other more mathematical approaches.

2. Derivation and structure

2.1. General background

Continuum models for surface growth are comparable to the hydrodynamic limit of microscopic models of fluid dynamics. Behind the continuous macroscopic height field $h(\mathbf{x}, t)$ one has to imagine an ensemble of microscopic configurations which are locally in a steady state. Figure 1 illustrates this relationship. The local state is subject to changes on time scales, ideally longer than the relaxation times into those states, which leads to the dynamics of the height field.

The structure of the PDE governing the dynamics of $h(\mathbf{x}, t)$ reflects different elementary processes and their symmetries. In growth from molecular beam epitaxy there is

- a deposition flux $F_{\{h\}}(\mathbf{x}, t)$, i.e., the deposited volume per time and surface area,
- possibly an evaporation loss $E_{\{h\}}(\mathbf{x}, t)$, again volume per time and area,
- a surface current $\mathbf{J}_{\{h\}}(\mathbf{x}, t)$ on terraces and along steps, transported volume per time and length, i.e., cross section on the surface.

Multiplied with a volume density ρ these quantities become mass fluxes and currents. All three depend on the actual surface configuration h , e.g., on local slopes, their orientations and curvatures. Elastic interactions and terrace adatom detachment with subsequent redeposition couple the dynamics at a surface point *non-locally* to surface configurations at other places. There may also be an *explicit* space dependence beyond the influence of the height configuration, e.g., for a non-uniform deposition with pulsed flux.

Deposition, evaporation, and surface current are combined into a *continuity equation*

$$\frac{\partial}{\partial t} h(\mathbf{x}, t) = F_{\{h\}}(\mathbf{x}, t) - \nabla \cdot \mathbf{J}_{\{h\}}(\mathbf{x}, t) - E_{\{h\}}(\mathbf{x}, t). \quad (2.1)$$

Note that small local slopes are assumed, such that any geometric prefactors to the divergence of the surface current typically are neglected.

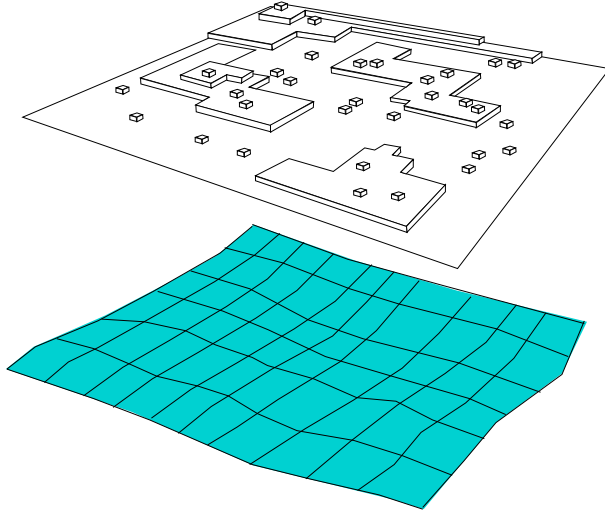


FIGURE 1. Sketch of the height field representation for surface configurations. Upper: one surface configuration out of an ensemble in local steady states. Lower: a smooth height field $h(\mathbf{x}, t)$ as a representation.

A full derivation from local steady states in the sense postulated above is of course impossible in almost any case, apart from some one-dimensional examples [3]. One therefore has to rely on heuristically justified (*reasonable*) assumptions for the dynamic quantities involved. The connection to the more detailed models on smaller scales is given by length scales which influence the surface morphology and become visible. Explained more precisely in the other introductory lectures of this conference [1, 10] they are

- a , the lattice spacing of the crystal.
- ℓ_D , the diffusion length, i.e., the “typical” distance of nucleation sites on a terrace, with a non-trivial dependence on the deposition rate F and adatom diffusivity D .
- ℓ_{ES} , the Ehrlich–Schwoebel length, i.e., a measure for the reflectivity of the barrier at a downward step. Roughly speaking, an adatom located right at a downward step is equally likely to hop downward as it is to reach the next upward step, if it lies at a distance ℓ_{ES} .
- ℓ_{step} , the average distance between two truly ascending at a vicinal surface of slope a/ℓ_{step} without counting islands between them.

2.2. Surface current

Ehrlich–Schwoebel effect on terraces

As was realised quite early the most important ingredient of Eq. (2.1) is a non-equilibrium current on surface terraces induced by Ehrlich–Schwoebel (ES) barriers [5, 18, 19, 23].

For small average slopes $\mathbf{m} = \nabla h$ with $|\mathbf{m}| \ll a/\ell_D$ or $\ell_D \ll \ell_{\text{step}}$, the ES barrier induces a net uphill current $\mathbf{J}_{\text{EST}} \sim F\mathbf{m}$. Inserted into the surface current in Eq. (2.1) this results in a *destabilising* term for the height equation $\partial_t h = -c\nabla \cdot \nabla h + \dots$

Of course one would like to know the functional dependence of the surface current \mathbf{J}_{EST} beyond this approximation for small slopes. Following an argument of Siegert for 1+1 dimensions [19] there must also be surface orientations with stabilising surface current: Think of \mathbf{J}_{EST} as a vector field on the tangent bundle of the unit sphere of possible surface orientations. By the ES instability all high symmetry orientations have \mathbf{J}_{EST} pointing outward around a zero. By continuity of \mathbf{J}_{EST} as a function of the orientation there must be zeroes with the current field pointing inward to the zero, i.e., orientations stabilised by the surface current.

These qualitatively fundamental properties, the existence of unstable and stable surface orientations, can be cast into a heuristically postulated function $\mathbf{J}_{\text{EST}}(\mathbf{m})$. Figure 2 shows two such examples, one isotropic within the crystal

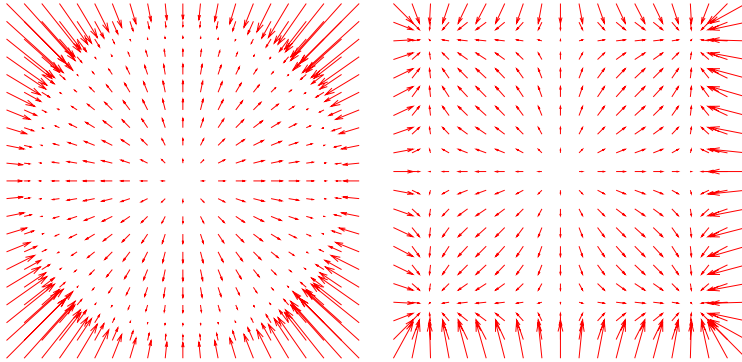


FIGURE 2. Examples of heuristic choices for nonequilibrium terrace Ehrlich-Schwoebel surface current $\mathbf{J}_{\text{EST}}(\mathbf{m})$. Left: in-plane isotropy, $\mathbf{J}_{\text{EST}}(\mathbf{m}) = (1 - |\mathbf{m}|^2) \mathbf{m}$, continuous set of stable slopes $\{\mathbf{m} \mid |\mathbf{m}| = 1\}$. Right: anisotropy, four-fold symmetry, $J_{\text{EST},i}(\mathbf{m}) = (1 - m_i^2) m_i$ with $i = x, y$, discrete set of stable slopes at $(\pm 1, \pm 1)$.

terrace — a somewhat artificial but nevertheless theoretically interesting case, one isotropic, with four-fold ($\pi/2$) rotational symmetry.

Ehrlich–Schwoebel effect at steps

The Ehrlich–Schwoebel effect also has an influence on adatom diffusion along steps, allowing for attachment of atoms to kinks preferentially from one side, as is sketched in Fig. 3. It is one important mechanism causing a step meandering

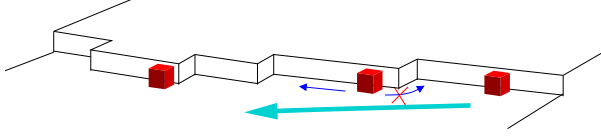


FIGURE 3. The ES effect at step kinks favours adatom incorporation from one side and induces a net current along the step.

instability on growing vicinal surfaces [13, 7]. Politi and Krug derived the contribution \mathbf{J}_{ESS} of non-equilibrium current along steps to the total surface current for a surface with given average slope which is assumed to be constant on a sufficiently large region such that steps have a well defined average density and orientation with respect to the underlying crystal lattice [15].

Curvature relaxation

Clearly on small scales the destabilising ES effects encountered in this section so far are balanced. Too thin protrusions are forbidden by their cost in surface free energy. For thermal relaxation towards equilibrium the corresponding continuum dynamics are straightforward to derive. The surface free energy

$$\mathcal{F} = \int \gamma(\nabla h) \sqrt{1 + (\nabla h)^2} d^d x \quad (2.2)$$

weights each surface element by its orientation dependent contribution $\gamma(\nabla h)$. The gradient in chemical potential $\mu = \delta\mathcal{F}/\delta h$ drives the relaxational surface current which is also proportional to the (tensorial and orientation dependent) adatom mobility $\sigma(\nabla h)$. A linear expansion around a surface of constant slope $h = \mathbf{m} \cdot \mathbf{x}$ small enough to again neglect geometric effects [12, 23] yields

$$\mathbf{J}_{\text{CURV}} = \sigma \cdot \nabla \nabla \cdot [\gamma \mathbf{1} + (\nabla_{\mathbf{m}} \nabla_{\mathbf{m}} \gamma)] \cdot \nabla h. \quad (2.3)$$

The expression in square brackets is generally called the surface *stiffness*

$$\tilde{\gamma} = \gamma \mathbf{1} + \nabla_{\mathbf{m}} \nabla_{\mathbf{m}} \gamma \quad (2.4)$$

where $\nabla_{\mathbf{m}}$ denotes derivation with respect to the slope dependence of γ and $\mathbf{1}$ is the unity matrix.

Strictly speaking this derivation applies only to *equilibrium relaxation*. For a far from equilibrium process like MBE growth it does not make sense to define a surface free energy per area $\gamma(\nabla h)$, although the “true” contribution of the surface current due to relaxation by curvature most likely has a functional form of that type. The identification of these contributions and the correct derivation of the corresponding continuum form remains an open question.

2.3. Deposition, desorption and noise

For most applications it will be correct to assume a *deposition* intensity F constant in time and space. Interesting cases with *explicit* space and time dependence are (i) pulsed molecular beams, used to decrease the second layer island nucleation rate, and (ii) geometric inhomogeneities if the beam does not reach every part of the surface under the same angle. The most important mechanism for *implicit* deposition heterogeneity is steering, where the incident atoms are deflected by attractive interaction with surface features such as islands and mounds, and effect which is of course most prominent under grazing incidence [4, 25].

At sufficiently high temperatures *desorption* may become an important effect. Terrace adatoms then will be most susceptible to desorption at a rate $1/\tau$, during their diffusion time before they reach the stronger binding steps. To a first approximation the desorption rate depends on the average distance to the next reachable step and therefore on the surface slope: the higher the slope, the more steps are present and the lower the desorption loss. Within an ansatz à la Burton–Cabrera–Frank [2] one can relate the desorption length $x_s = 2a\sqrt{D\tau}$, diffusion length ℓ_D , and slope $\nabla h = a/\ell$ [21, 23] to an expression for the desorption loss in volume per time and surface area

$$E_{\{h\}}(\mathbf{x}, t) = F [(x_s/\ell) \tanh(\ell/x_s) - 1] \approx F \frac{(\ell_D/x_s)^2/3}{1 + (\nabla h)^2}. \quad (2.5)$$

There are three sources for *noise* in MBE growth [24]: (i) Deposition is a stochastic process of single events, so F has to be complemented by a “shot noise” term $\xi(\mathbf{x}, t)$ with statistics

$$\langle \xi(\mathbf{x}, t) \rangle = 0 \quad \text{and} \quad \langle \xi(\mathbf{x}, t) \xi(\mathbf{x}', t') \rangle = a^3 F \delta(\mathbf{x} - \mathbf{x}') \delta(t - t'). \quad (2.6)$$

(ii) Adatom diffusion also consists of single events, and to a first approximation surface currents are blurred by a “diffusion noise” term $\boldsymbol{\eta}(\mathbf{x}, t)$ with statistics

$$\langle \boldsymbol{\eta}(\mathbf{x}, t) \rangle = 0 \quad \text{and} \quad \langle \boldsymbol{\eta}(\mathbf{x}, t) \cdot \boldsymbol{\eta}(\mathbf{x}', t') \rangle = \ell_D F \nabla^2 \delta(\mathbf{x} - \mathbf{x}') \delta(t - t'). \quad (2.7)$$

(iii) Nucleations also occur at random but the precise form of this contribution remains an open question. There are nontrivial correlations in time, as new islands tend to nucleate close to centres of previously nucleated islands. The space dependence of the nucleation noise correlator $\langle \nu(\mathbf{x}, t) \nu(\mathbf{x}', t') \rangle$ is expected to have the form $(\nabla^2)^2 \delta(\mathbf{x} - \mathbf{x}')$ [22].

2.4. Structure and symmetry of continuum equations for MBE

Heuristic surface currents as in the example in Fig. 2 lead to a symmetry in the resulting dynamical equation which can be used for evaluation, but is too strong a restriction compared to the “real” dynamics and may lead to erroneous results.

If \mathbf{J}_{EST} uniquely depends on the slope \mathbf{m} and not on derivative of its functions then crystal symmetry imposes $\mathbf{J}_{\text{EST}}(\mathbf{m}) = -\mathbf{J}_{\text{EST}}(-\mathbf{m})$. The resulting term of surface dynamics is invariant under the transformation $h \rightarrow -h$ and so will be the surface configurations obtained from that. Breaking of this symmetry, e.g., by

terms as $\nabla f((\nabla h)^2)$ in \mathbf{J} or an evaporation term $e((\nabla h)^2)$ do in fact change the characteristics of the dynamics substantially [21, 11]

One can take advantage of this simple slope dependence if there is a scalar function $V(\mathbf{m})$ such that $\mathbf{J}_{\text{EST}} = -\nabla_{\mathbf{m}}V(\mathbf{m})$. Stable zeroes of \mathbf{J}_{EST} then are minima of $V(\mathbf{m})$. If additionally the curvature relaxation is of a simple ‘‘scalar’’ form $\boldsymbol{\sigma} \cdot \tilde{\boldsymbol{\gamma}} = K\mathbf{1}$ there is a Lyapunov functional of the dynamics

$$\mathcal{F}\{\mathbf{m}\} = \int \left[\frac{K}{2}(\nabla\mathbf{m})^2 + V(\mathbf{m}) \right] d^2x \quad (2.8)$$

and the surface dynamics Eq. (2.1) can be written for the field of slopes $\mathbf{m} = \nabla h$ as

$$\partial_t \mathbf{m} = \partial_t(\nabla h) = \nabla \nabla \cdot \frac{\delta \mathcal{F}}{\delta \mathbf{m}}. \quad (2.9)$$

If \mathbf{m} is interpreted as a two-dimensional magnetic order parameter this from compares to conserved (model B) relaxational dynamics, with the only restriction that it remains a conservative field at all times, $\nabla \wedge \mathbf{m} = 0$. Facets in the surface are regions of constant slope, and appear as domains of constant ‘‘magnetisation’’, edges between them are domain walls. As compared to its magnetic analogon, here the parallel component of \mathbf{m} remains constant across a domain wall, which in the case of discrete stable zeroes of the current function (right panel of Fig. 2) restricts the possible domain wall orientations and imposing constraints on the relaxational dynamics [11, 19, 20].

3. Examples of applications

Continuum equations are now applied in two examples of very basic choices in Eq. (2.1). In some sense they highlight two opposite regimes, (i) on very long length and time scales coarsening of mounds in homoepitaxy, and (ii) on short scales resolving the lattice structure in the transition from layer-by-layer to rough growth.

3.1. Coarsening

In some sense the simplest example of a surface dynamics equation is the analogon to the classical XY-model in the sense of Eq. (2.9)

$$\partial_t h = -(\nabla^2)^2 h - \nabla \cdot [(1 - (\nabla h)^2) \nabla h], \quad (3.1)$$

i.e., with the current function depicted in the left panel of Fig. 2. An initially flat surface $h = \text{const}$ is linearly unstable to fluctuations of wave lengths $\lambda > 2\pi$ which therefore initially grow exponentially. Once slopes of $O(1)$ are reached the surface organises itself into a pattern of regular mounds and troughs which keep the symmetry $h \leftrightarrow -h$ of Eq. (3.1). The in-plane isotropy of (3.1) is locally broken by the need to arrange the mounds and troughs into a regular pattern and facets with sharp wedges form [14].

Subsequently the pattern of mounds and troughs coarsens keeping a single typical length scale and a statistically self similar pattern at every time. The

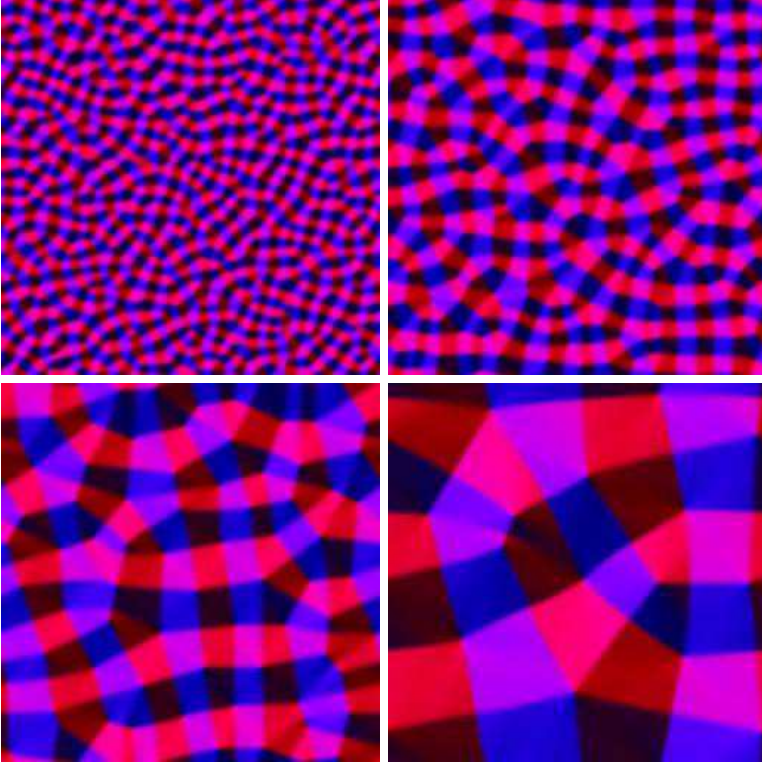


FIGURE 4. Coarsening of surface mounds, between subsequent panels time advances by a factor of 10. The local surface slope is represented by colours, facets appear as regions of uniform colour. Spontaneous facet formation, although no anisotropy is imposed, $\mathbf{J}_{\text{EST}}(\mathbf{m}) = (1 - |\mathbf{m}|^2) \mathbf{m}$ (c.f. left panel in Fig. 2).

average mound size is found to increase with time as $L \sim t^{1/3}$ [11, 20]. In a weak sense this can be proved as an upper bound for an appropriate time average of the length scales L observed up to a given time t [9]. Here only a quick handwaving argument is given following [16]:

The spatial average of the interface width $W \equiv \langle h^2 \rangle$ (where $\langle h \rangle = 0$) increases due to Eq. (3.1) as

$$\frac{1}{2} \partial_t W^2 = \frac{1}{2} \partial_t \langle h^2 \rangle = -\langle (\Delta h)^2 \rangle + \langle (\nabla h)^2 \rangle - \langle |\nabla h|^4 \rangle. \quad (3.2)$$

By the sketch of Fig. 3.1 the contributions of these terms are estimated to be of order $1/L$: The facets are flat and the curvature is restricted to narrow strips of width $O(1)$ at the domain boundaries, which have a relative weight of $1/L$. Also, here the slopes are smaller than the stable value $|\nabla h| = 1$ attained at the facets.

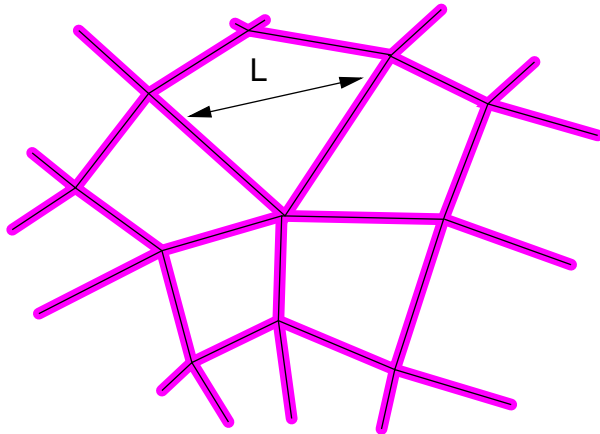


FIGURE 5. Sketch of facets and wedges, i.e., domains of constant slope and their separating boundaries, as obtained in the simulations shown in Fig. 2.4. The only macroscopic length scale is the domain size L .

So all terms give a contribution of $O(1/L)$ and because of the stable slope $W \sim L$ the increase in width leads to the estimate

$$\partial_t L^2 \sim \partial_t W^2 \sim 1/L, \quad \text{integrated to } L \sim t^{1/3}. \quad (3.3)$$

The same rough heuristic argument holds for anisotropic surface currents with discrete minima, i.e., a discrete set of preferential surface orientations, but the four-fold symmetry (right panel of Fig. 2) plays a special role because two kinds of edges occur, such that in general the assumption of a single length scale L in the system is wrong [20].

3.2. Roughening

Layer by layer growth is technologically interesting because one can monitor the subsequent deposition of layers by oscillations in the surface width. It is nearly flat around integer fillings and the roughness takes maxima at half integer fillings. During growth the interface roughens and the width oscillations decay [6]. The Ehrlich–Schwoebel barrier and mounding instability is one prominent mechanism destroying layer-by-layer growth, and so can be any inhomogeneity in the deposition intensity $F_{\{h\}}(\mathbf{x}, t)$. Although weaker, even the fluctuations of shot noise have this effect, and it can be captured by a simple renormalisation group calculation.

The simplest way to implement layer lattice effects into an continuum surface equation like Eq. (2.1) is pursued by the conserved *sine-Gordon*-equation

$$\partial_t h(\mathbf{x}, t) = -K \Delta^2 h(\mathbf{x}, t) - V \Delta \sin \frac{2\pi h(\mathbf{x}, t)}{a_\perp} + F + \xi(\mathbf{x}, t). \quad (3.4)$$

Among other the surface current is driven to regions of incomplete fillings such that $h(\mathbf{x}, t)/a_{\perp}$ is favoured to take integer values [17]. The notation distinguishes between the lattice constant normal (a_{\perp}) and parallel (a_{\parallel}) to the surface terraces which will be used in the following analysis.

In a momentum shell renormalisation one can average over the fluctuations caused by the short wavelength components of the noise, $\xi = \bar{\xi} + \delta\xi$, where $\bar{\xi}$ only contains modes of wavenumber smaller than some cutoff Λ and $\delta\xi$ the others. One now tries to approximate the dynamic equation for the averaged height field $\bar{h} = \langle h \rangle_{\delta\xi}$ by an equation like (3.4) with suitably adjusted parameters. After rescaling, an effective *renormalised* equation is obtained. Three important physical interpretations can be obtained from the renormalised parameters of Eq. (3.4).

(i) by the interplay of the diving force F and the lattice potential the up-down symmetry ($h \leftrightarrow -h$) is broken and a term $-\lambda\Delta(\nabla h)^2$ is created.

(ii) The strength of the lattice potential V is damped out decays exponentially with coverage $\theta = Ft$ like $\propto \exp\left(-a_{\parallel}^2/\ell_D^2\sqrt{\theta}\right)$

(iii) In a finite size sample smaller than the so called *layer coherence* length $\tilde{\ell} = \ell_D^2/a_{\parallel}$ renormalisation has to stop before the lattice potential has decayed. Shot noise fluctuations cannot accumulate to the point where width oscillations are completely blurred.

4. Discussion

In presenting the model derivations and examples of their application it becomes clear that continuum models are a good tool for questions where the inherent *simplifications* are justified. The insight gained from partial differential equations is different from results of more microscopic model. Last not least continuum equations can handle larger systems and longer times than Monte Carlo simulations or even Molecular Dynamics.

In many cases the phenomena of particular technological interest cannot be captured by continuum equations of the type described in this lecture. Magic island shapes, surface reconstruction, step bunching, formation of quantum dots and wires are just a few examples.

Even if one isn't interested in these inherently discrete phenomena themselves they nevertheless carry over to the behaviour on larger scales and a naive straightforward derivation of large scale continuum models may be wrong. The implementation of noise for some questions, such as roughening, is one such example. Also, the effective "large scale" Ehrlich-Schwoebel barrier of a step is influenced by kinks along the step which may serve as channels for downward incorporation of a terrace adatom. Obtaining the correct effective barrier, dependent on orientation and curvature of the step certainly is a nontrivial task.

An important part of the surface current \mathbf{J} flows along steps, as has become clear in the above derivation. In ref. [15] the step current due to kink ES barriers

is derived as a function of the surface orientation or slope. An open question is the role of step curvature and therefore of surface curvature on the step current.

Also on the surface itself, the regularising term as it is derived in Eq. (2.3), should be derived from true nonequilibrium arguments. To do so, one would have to incorporate island nucleations, the creation and annihilation of steps. One possible approach is to introduce fields for the densities of adatoms, advacancies, steps, kinks, and for their orientations. Locally they could be treated as mean field densities with certain effective “reaction” rates, but in their spatial interaction, by diffusion and advective transport, one could obtain a conceptually more fundamental continuum model for surface growth.

5. Conclusion

In this lecture an overview of continuum models for MBE surface growth has been given which includes

- the conceptual foundation of continuum models as a limit of more detailed small scale approaches,
- heuristic derivations due to lack of rigorous or even exact ways to obtain them,
- the structure and the symmetry of the equations obtained in that way,
- two examples emphasising two opposite time limits in the growth process with the application of two contrary methods,
- criticism of weak points in continuum modelling, open questions and some speculations about answers to them.

The main purpose was to highlight the physical background and give some intuition of possible approaches to it as a basis for mathematical treatments, both rigorous and numerical. It should be seen as a complement of the lectures [1] and [10] which give a similar introduction to lattice and Burton–Cabrera–Frank models respectively. Although continuum models seem to fail in some important physical aspects they nevertheless are a good tool and subject for mathematical approaches.

References

- [1] M. Biehl (2004) this volume.
- [2] W.K. Burton, N. Cabrera, F.C. Frank, *The growth of crystals and the equilibrium of their surfaces*, Phil. Trans. Roy. Soc. London A **243** (1951) 299–358.
- [3] B. Derrida, E. Domany, and D. Mukamel, *An exact solution of the one dimensional asymmetric exclusion model with open boundaries*, J. Stat. Phys. **69** (1992) 667–687; G. Schütz and E. Domany, *Phase transitions in an exactly soluble one-dimensional asymmetric exclusion model*, J. Stat. Phys. **72** (1993) 277–296.
- [4] S. van Dijken, L.C. Jorritsma, and B. Poelsema, *Steering-Enhanced Roughening during Metal Deposition at Grazing Incidence*, Phys. Rev. Lett. **82** (1999) 4038–4041.

- [5] G. Ehrlich and F.G. Hudda, *Atomic view of surface diffusion: Tungsten on Tungsten*, J. Chem. Phys. **44** (1966) 1036–1099.
- [6] H. Kallabis, L. Brendel, J. Krug, J., and D.E. Wolf, *Damping of oscillations in layer-by-layer growth*, Int. J. Mod. Phys. B **31** (1997) 3621–3634.
- [7] J. Kallunki, J. Krug, M. Kotrla, *Competing mechanisms for step meandering in unstable growth*, Phys. Rev. B **65** (2002) 205411.
- [8] R.V. Kohn and F. Otto, *Upper bounds on coarsening rates*, Comm. Math. Phys. **229** (2002) 375–395.
- [9] R.V. Kohn, X.D. Yan, *Upper bound on the coarsening rate for an epitaxial growth model*, Comm. Pure Appl. Math. **56** (2003) 1549–1564.
- [10] J. Krug (2004) this volume.
- [11] D. Moldovan and L. Golubovic, *Interfacial coarsening dynamics in epitaxial growth with slope selection*, Phys. Rev. E **61** (2000) 6190–6214.
- [12] W.W. Mullins, *Flattening of a Nearly Planar Solid Surface Due to Capillarity*, J. Appl. Phys. **30** (1959) 77–??.
- [13] O. Pierre-Louis, M.R. D’Orsogna, and T.L. Einstein, *Edge diffusion during growth: The kink Ehrlich-Schwoebel effect and resulting instabilities*, Phys. Rev. Lett. **82** (1999) 3661–3664.
- [14] P. Politi, G. Grenet, A. Marty, A. Ponchet, and J. Villain, *Instabilities in crystal growth by atomic or molecular beams*, Physics Reports **324** (2000) 271–404.
- [15] P. Politi and J. Krug, *Crystal symmetry, step-edge diffusion, and unstable growth*, Surface Science **446** (2000) 89–97.
- [16] M. Rost and J. Krug *Coarsening of surface structures in unstable epitaxial growth*, Phys. Rev. E **55** (1997) 3952–3957.
- [17] M. Rost and J. Krug, *Damping of growth oscillations in molecular beam epitaxy: A renormalization group approach*, J. de Physique I **7** (1997) 1627–1638.
- [18] L. Schwoebel and E.J. Shipsey, *Step motion on crystal surfaces*, J. Appl. Phys. **37** (1966) 3682–3686.
- [19] M. Siegert, *Ordering dynamics of surfaces in molecular beam epitaxy*, Physica A **239** (1997) 420–427.
- [20] M. Siegert, *Coarsening dynamics of crystalline thin films*, Phys. Rev. Lett. **81** (1998) 5481–5484.
- [21] P. Šmilauer, M. Rost, and J. Krug, *Fast coarsening in unstable epitaxy with desorption*, Phys. Rev. E **59** (1999) R6263–R6266.
- [22] E. Somfai, D.E. Wolf, and J. Kertész, *Correlated island nucleation in layer-by-layer growth*, J. de Physique I **6** (1996) 393–401.
- [23] J. Villain, *Continuum models of crystal growth from atomistic beams with and without desorption*, J. de Physique I **1** (1991) 19–42.
- [24] D.E. Wolf, *Computer simulation of molecular-beam epitaxy*, in *Scale Invariance, Interfaces and Non-Equilibrium Dynamics*, Eds. A.J. McKane, M. Droz, J. Vannimenus, and D.E. Wolf, Plenum Press, New York (1995).
- [25] J. Yu, J.G. Amar, and A. Bogicevic, *First-principles calculations of steering forces in epitaxial growth*, Phys. Rev. B **69** (2004) 113406.

Acknowledgement

This work, as well as the participation at the workshop was supported by SFB 611 (Singuläre Phänomene und Skalierung in mathematischen Modellen) of Deutsche Forschungsgemeinschaft.

Martin Rost
Bereich Theoretische Biologie
Insitut für Zelluläre und Molekulare Botanik
Kirschallee 1, Universität Bonn
53115 Bonn, Germany
e-mail: martin.rost@uni-bonn.de